IOPscience iopscience.iop.org

Home Search Collections Journals About Contact us My IOPscience

Measurement of the thickness distribution and optical constants of non-uniform thin films

This article has been downloaded from IOPscience. Please scroll down to see the full text article.

2011 Meas. Sci. Technol. 22 085104

(http://iopscience.iop.org/0957-0233/22/8/085104)

View the table of contents for this issue, or go to the journal homepage for more

Download details:
IP Address: 141.53.32.57
The article was downloaded on 11/07/2011 at 15:07

Please note that terms and conditions apply.

Meas. Sci. Technol. **22** (2011) 085104 (8pp) doi:10.1088/0957-0233/22/8/085104

# Measurement of the thickness distribution and optical constants of non-uniform thin films

**M Ohlídal[1], I Ohlídal[2], P Klapetek[3], D Nečas[2] and A Majumdar[4]**

[1] Institute of Physical Engineering, Brno University of Technology, Brno, Czech Republic
[2] Faculty of Science, Department of Physical Electronics, Masaryk University, Brno, Czech Republic
[3] Czech Metrology Institute, Brno, Czech Republic
[4] Institute of Physics, University of Greifswald, Greifswald, Germany

E-mail: ohlidal@fme.vutbr.cz (M Ohlídal)

Received 29 December 2010, in final form 9 May 2011
Published 28 June 2011
Online at stacks.iop.org/MST/22/085104

**Abstract**

In this paper, an original method for the complete optical characterization of thin films exhibiting area thickness non-uniformity is presented. This method is based on interpreting experimental data obtained using an original imaging spectroscopic photometer operating in the reflection mode at normal incidence of light. A CCD camera is employed as a detector of the photometer. The spectral dependences of the reflectance measured simultaneously by individual pixels of the CCD camera correspond to the local reflectance of small areas of the non-uniform thin films characterized. These areas form a matrix along a relatively large part of the substrate covered with the non-uniform film. The spectral dependences of the local reflectance measured by the individual pixels are treated separately by means of the formulae for the reflectance valid for uniform thin films. The reason is that the local areas corresponding to the pixels are sufficiently small so that the film characterized can be considered to be uniform within these local areas. Using this approach, it is possible to determine the values of the local thickness and local optical constants for every small area of the matrix. Thus, in principle it is possible to determine the distributions (maps) of the local thickness and the local optical constants of the non-uniform films simultaneously. This method is used to characterize carbon-nitride thin films exhibiting only the thickness area non-uniformity.

**Keywords:** non-uniform thin films, imaging spectroscopic reflectometry, distribution of the local thickness

(Some figures in this article are in colour only in the electronic version)

## 1. Introduction

Thin films are utilized very frequently in practice. Many of them exhibit area non-uniformity. For example, thin films prepared by various plasma-chemical methods often exhibit area non-uniformity in the optical parameters, i.e. in the optical constants and thickness. It is known that the existence of this non-uniformity can strongly influence the properties of the thin films (see e.g. [1–6]). Moreover, area non-uniformity can misrepresent the results of the characterization of thin films if this non-uniformity is not taken into account (see e.g. [1, 2, 4, 7]).

It is very difficult to perform a correct optical characterization of non-uniform films by means of the standard optical methods employed most frequently in practice (e.g. photometric and ellipsometric methods [4, 7–9]). In many cases of non-uniform thin films, the standard photometric and ellipsometric methods cannot be used at all. Therefore, it is necessary to develop new optical methods enabling us to perform a complete optical characterization of films

 © 2011 IOP Publishing Ltd Printed in the UK & the USA

non-uniform in thickness and optical constants with sufficient precision.

Imaging spectroscopic reflectometry (ISR) represents such a new approach. Within the scope of this technique, we developed a new method allowing us to perform the complete optical characterization of non-uniform absorbing thin films. Using this ISR method, it is possible to determine the area thickness distribution along these non-uniform films together with the area distribution of the spectral dependences of their optical constants if a suitable dispersion model of these optical constants is selected. In principle, an important advantage of ISR consists in the possibility of using the formulae corresponding to uniform thin films in the treatment of experimental data. This ISR method is applied using an imaging spectroscopic photometer (ISP) containing a CCD camera as a detector. We developed an original ISP that can be employed in both reflection and transmission modes [10]. This ISP is a two-channel instrument operating in *ex situ* mode in contrast to a one-channel ISP operating in *in situ* mode utilized for technological purposes [11].

In this paper, ISR is applied to non-uniform carbon-nitride films because these films prepared by plasma-enhanced chemical vapor evaporation deposition (PECVD) exhibit relatively strong thickness non-uniformity along the surfaces of silicon single substrates [7].

## 2. Experimental part

### *2.1. Sample preparation*

The non-uniform carbon-nitride films were deposited by dielectric barrier discharge with $CH_4/N_2$ gas mixture onto silicon single crystal wafers at a pressure within a range from 300 to 400 mbar. The details of preparing the carbon-nitride films are described in [3]. Note that the carbon-nitride films prepared in this way exhibited amorphous structure.

### *2.2. Experiment setup*

A schematic diagram of the ISP employed is presented in figure 1.

The detector in the sample channel of the ISP is a CCD camera (Hamamatsu Digital CCD Camera Orca-II C4742-98-26AG) and so the spectral local reflectances of small areas on the non-uniform thin film corresponding to the individual pixels of this camera are measured. Thus, the spectral local reflectances are measured in the small areas forming a matrix on this film. A sample holder is constructed in such a way that the normal reflectance of the films is measured in the individual pixels of the CCD camera within a range of 320–810 nm. The concrete procedure for measuring the local reflectance $R^{k,u}$ corresponding to the individual elements of the matrix, i.e. corresponding to the individual pixels, is described in our earlier paper [10]. A very important part of it is a proper adjustment of samples. It is necessary to ensure the identical angular position of the studied and the reference samples. We achieve this using the beam of an

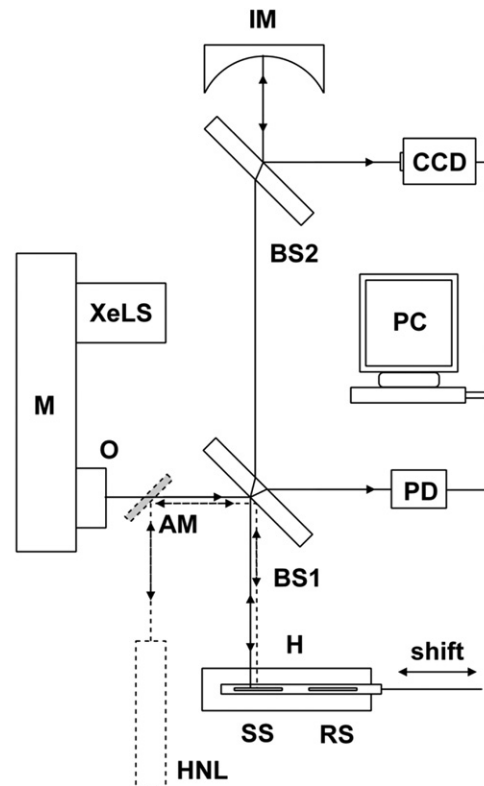


**Figure 1.** Schematic diagram of the ISR experiment setup: M—monochromator, XeLS—xenon light source, O—output of the monochromator, BS1, BS2—beam-splitters, IM—imaging mirror, CCD—CCD camera, PC—computer, H—holder of samples, SS—studied sample, RS—reference sample, PD—photodetector, HNL—helium–neon laser, AM—auxiliary mirror.

auxiliary He–Ne laser HNL and an auxiliary mirror AM (the dashed line in figure 1). The position of the beam on the output of the laser after its reflection on the mirror AM, beam-splitter BS1 and the samples must be the same in both cases. After finishing the adjustment of samples, the mirror AM is removed from its position. Further steps of the procedure are as follows.

(1) The reference sample RS is situated in the position of the measuring channel. The signal $S_{MR}^{k,u}(t_1, \lambda)$ recorded by the $(k, u)$th pixel of the CCD camera at time $t_1$ and wavelength $\lambda$ is determined in the following way:

$$S_{MR}^{k,u}(t_1, \lambda) = I_0(t_1, \lambda)\eta_M^{k,u}(\lambda)R_0^{k,u}(\lambda), \tag{1}$$

where the indices $(k, u)$ belong to the $(k, u)$th pixel ($k = 1, \ldots, A$; $u = 1, \ldots, B$, where $A$ and $B$ are integers), $I_0(t_1, \lambda)$ is the intensity of the output beam of the monochromator at time $t_1$ and wavelength $\lambda$, $\eta_M^{k,u}(\lambda)$ is the so-called apparatus function for the measuring channel of the experiment setup corresponding to the $(k, u)$th pixel (it includes the influence of the quartz wedge-shaped beam-splitters BS1, BS2, the spherical imaging mirror IM and the parameters of the CCD camera) and $R_0^{k,u}(\lambda)$ is the local absolute reflectance of the reference sample corresponding to the $(k, u)$th pixel. In practice, one can select the reference samples, such

as a silicon single-crystal wafer for which it holds that $R_0^{k,u}(\lambda) = R_0(\lambda)$. The signals $S_{MR}^{k,u}(t_1, \lambda)$ create the image of the reference sample for the wavelength $\lambda$ at time $t_1$.

At the same time $t_1$ and the same wavelength $\lambda$, the signal $S_{RR}(t_1, \lambda)$ is recorded by the integrating photodetector PD (Hamamatsu Si photodiode S1226-8BQ/-8BK) in the reference channel:

$$S_{RR}(t_1, \lambda) = I_0(t_1, \lambda)\eta_R(\lambda), \tag{2}$$

where $\eta_R(\lambda)$ is the apparatus function for the reference channel of the experiment setup. It includes the influence of the beam-splitter BS1 and the parameters of the photodetector PD. The signals $S_{MR}^{k,u}(t_1, \lambda)$ and $S_{RR}(t_1, \lambda)$ appearing in (1) and (2) are measured at a sufficient number of wavelengths from the spectral range of interest.

(2) The sample measured SS is situated in the position of the measuring channel. Then the steps of the measurements described above are repeated with this sample. Of course, these measuring steps must be performed at the same wavelength as for the reference sample. In this way, we obtain the following equations for the signals detected by the individual pixels of the CCD camera $S_{MS}^{k,u}(t_2, \lambda)$ and the integrating photodetector $S_{RS}(t_2, \lambda)$ at time $t_2$:

$$S_{MS}^{k,u}(t_2, \lambda) = I_0(t_2, \lambda)\eta_M^{k,u}(\lambda)R^{k,u}(\lambda) \tag{3}$$

$$S_{RS}(t_2, \lambda) = I_0(t_2, \lambda)\eta_R(\lambda), \tag{4}$$

where $R^{k,u}(\lambda)$ is the local absolute reflectance of the studied sample corresponding to the ($k$, $u$)th pixel. The signals $S_{MS}^{k,u}(t_2, \lambda)$ create the image of the studied sample for the wavelength $\lambda$ at time $t_2$.

(3) The values of the ratio $P_R^{k,u}(t_1, \lambda)$ corresponding to situating the reference sample into the measuring channel at time $t_1$ are determined in the following way:

$$P_R^{k,u}(t_1, \lambda) = \frac{S_{MR}^{k,u}(t_1, \lambda)}{S_{RR}(t_1, \lambda)} = \frac{\eta_M^{k,u}(\lambda)}{\eta_R(\lambda)} R_0(\lambda). \tag{5}$$

Similarly we obtain an analogous ratio $P_S^{k,u}(t_2, \lambda)$ of the signals for the situation when the studied sample is placed into the measuring channel at time $t_2$:

$$P_S^{k,u}(t_2, \lambda) = \frac{S_{MS}^{k,u}(t_2, \lambda)}{S_{RS}(t_2, \lambda)} = P_R^{k,u}(t_1, \lambda)\frac{R^{k,u}(\lambda)}{R_0(\lambda)}. \tag{6}$$

In conclusion, we find

$$R^{k,u}(\lambda) = \frac{P_S^{k,u}(t_2, \lambda)}{P_R^{k,u}(t_1, \lambda)} R_0(\lambda). \tag{7}$$

Using the arrangement described, it is possible to determine the spectral dependence of the local relative reflectance $R^{k,u}(\lambda)/R_0(\lambda)$ of the studied sample corresponding to each pixel of the CCD camera owing to the reference sample since the ratios $P_S^{k,u}(t_2, \lambda)$ and $P_R^{k,u}(t_1, \lambda)$ are determined by means of this arrangement quantitatively. Because the absolute reflectance $R_0(\lambda)$ of the reference sample is known, it is possible to determine the local absolute reflectance of the sample measured corresponding to all the pixels too.

## 3. Data processing

The area of the non-uniform thin films imaged by our spectrophotometer onto one pixel of the CCD camera is a square of 37 × 37 $\mu$m$^2$. The majority of thin films non-uniform in thickness exhibit such a gradient of the thickness distribution so that within this area these films can be considered uniform in thickness. Only for the films having extremely strong thickness non-uniformity is this assumption not valid. Thus, for the majority of non-uniform thin films, it is possible to suppose that the local reflectance $R^{k,u}$ measured by an individual pixel is expressed by the known formulae valid for uniform thin films. This means that the local reflectance $R^{k,u}$ is given by the following formulae [12, 13]:

$$R^{k,u} = |\hat{r}^{k,u}|^2, \tag{8}$$

where

$$\hat{r}^{k,u} = \frac{\hat{r}_1^{k,u} + \hat{r}_2^{k,u}\exp(\mathrm{i}\hat{x}^{k,u})}{1 + \hat{r}_1^{k,u}\hat{r}_2^{k,u}\exp(\mathrm{i}\hat{x}^{k,u})}, \tag{9}$$

$$\hat{r}_1^{k,u} = \frac{n_0 - \hat{n}_1^{k,u}}{n_0 + \hat{n}_1^{k,u}}, \tag{10}$$

$$\hat{r}_2^{k,u} = \frac{\hat{n}_1^{k,u} - \hat{n}}{\hat{n}_1^{k,u} + \hat{n}}, \tag{11}$$

$$\hat{x}^{k,u} = \frac{4\pi}{\lambda}\hat{n}_1^{k,u}d_1^{k,u}. \tag{12}$$

In the foregoing equations, the symbols $n_0$, $\hat{n}$, $\hat{n}_1^{k,u}$, $d_1^{k,u}$ and $\lambda$ denote the refractive index of the ambient, complex refractive index of the substrate, local complex refractive index of the film, local thickness of the film and wavelength of incident light, respectively. Note that the ambient consists of air, and therefore $n_0 = 1$. The complex refractive index of the substrate and/or film is expressed as $\hat{n} = n_s + \mathrm{i}k_s$ and/or $\hat{n}_1 = n_1 + \mathrm{i}k_1$. The symbols $n_s$ and $k_s$ are the real refractive index and extinction coefficient of the substrate, respectively, and the symbols $n_1$ and $k_1$ denote the refractive index and extinction coefficient of the film, respectively. The foregoing mathematical expressions for the local reflectance $R^{k,u}$ belonging to the individual pixels of the CCD camera correspond to the reflectance of the absorbing thin film deposited onto an absorbing substrate. Strictly speaking, the optical model of the isotropic homogeneous absorbing substrate covered with an isotropic homogeneous absorbing thin film was thus employed for expressing the local reflectance corresponding to the individual pixels of the CCD chip.

The least-squares method (LSM) was used to treat the experimental data using (8). Of course, the LSM had to be applied for each local area on the film corresponding to the

given pixel of the CCD camera. Within the LSM, the following merit function $S^{k,u}$ was employed:

$$S^{k,u} = \sum_{s=1}^{K} \left( \frac{R_s^{k,u} - R_s^{\prime k,u}}{\sigma_s^{k,u}} \right)^2, \qquad (13)$$

where $R_s^{k,u}$ and/or $R_s^{\prime k,u}$ denotes the theoretical and/or experimental value of the local reflectance corresponding to the $(k, u)$th pixel and wavelength $\lambda_s$. The symbol $\sigma_s^{k,u}$ and/or $K$ represents the standard deviation of $R_s^{\prime k,u}$ and/or the number of measurements of the local reflectance, i.e. the number of wavelengths, for which the local reflectance was measured by the individual pixels.

The dispersion model of the optical constants of the carbon-nitride thin films based on parameterization of the joint density of states (JDOS) was employed within the processing of the experimental data. The JDOS is defined, for example, in [14–16]. The detailed description of the parameterized joint density of states (PJDOS) model is presented in [17]. Within the PJDOS model, the imaginary part of the dielectric function $\varepsilon_i(E)$ is expressed using the following formula:

$$\varepsilon_i(E) = \frac{J(E)}{E^2} = \frac{1}{E^2} \sum_{j=1}^{N} J_{j\to j^*}(E), \qquad (14)$$

where $E$, $N$ and $J_{j\to j^*}(E)$ denote the photon energy, number of transitions and non-normalized JDOS corresponding to the $j \to j^*$ transition, respectively. The quantity $J_{j\to j^*}(E)$ is defined as follows [14–16]:

$$J_{j\to j^*}(E) = \left(\frac{eh}{m}\right)^2 \frac{|p_{j\to j^*}|^2}{4\pi\varepsilon_0 B_0} \Im_{j\to j^*}(E), \qquad (15)$$

where $e$, $h$, $m$, $\varepsilon_0$ and $B_0$ represent the electron charge, Planck's constant, electron mass, dielectric function of vacuum and a certain part of the Brillouin zone of the corresponding crystalline material, respectively. The symbol $|p_{j\to j^*}|^2$ denotes the squared momentum-matrix element. The symbol $\Im_{j\to j^*}(E)$ represents the JDOS function belonging to the $j \to j^*$ transition. The explicit expression of $\Im_{j\to j^*}(E)$ is given in [17]. The symbol $J(E)$ in (14) expresses a sum of the above-introduced $J_{j\to j^*}(E)$ corresponding to all the transitions in material forming the thin film.

The following parameterization of $J_{j\to j^*}(E)$ was employed:

$$J_{j\to j^*}(E) \propto (E - E_{gj})^2 (E - E_{hj})^2, \qquad (16)$$

where $E_{gj}$ and $E_{hj}$ denote the minimum energy limit (band gap) and maximum energy limit of the transition $j \to j^*$, respectively.

Note that the following equation is fulfilled [17]:

$$\int_0^\infty J_{j\to j^*}(E)\,\mathrm{d}E = Q_j^2 \qquad (17)$$

where $Q_j$ is the quantity proportional to the concentration of $j$ electrons in material.

From the foregoing, the following equation is derived:

$$\varepsilon_{i,j\to j^*}(E) = \frac{30 Q_j^2 (E - E_{gj})^2 (E - E_{hj})^2}{(E_{hj} - E_{gj})^5 E^2} \quad \text{for } E_{gj} \prec E \prec E_{hj} \qquad (18)$$

and

$$\varepsilon_{i,j\to j^*}(E) = 0 \qquad \text{for } E \text{ out of } E_{gj} \prec E \prec E_{hj}. \qquad (19)$$

Using the Kramers–Kronig relation [17], the contribution of the $j \to j^*$ transition to the real part of the dielectric function $\varepsilon_{r,j\to j^*}(E)$ could be analytically expressed as

$$\varepsilon_{r,j\to j^*}(E) = \kappa \left[ B \ln\left|\frac{E + E_{hj}}{E + E_{gj}}\right| + C \ln\left|\frac{E - E_{hj}}{E - E_{gj}}\right| - D \right], \qquad (20)$$

where

$$\kappa = \frac{60 Q_j^2}{\pi (E_{hj} - E_{gj})^5}, \qquad B = \frac{Y(E) + X(E)}{2E^2}, \qquad (21)$$

$$C = \frac{Y(E) - X(E)}{2E^2} \qquad (22)$$

$$D = \frac{E_{gj}^2 E_{hj}^2}{E^2} \ln\left|\frac{E_{hj}}{E_{gj}}\right| + \frac{3\left(E_{hj}^2 - E_{gj}^2\right)}{2} \qquad (23)$$

$$X(E) = 2E\left[E_{hj}\left(E_{gj}^2 + E^2\right) + E_{gj}\left(E_{hj}^2 + E^2\right)\right] \qquad (24)$$

and

$$Y(E) = E^2\left(E_{hj}^2 + E_{gj}^2 + 4E_{gj}E_{hj} + E^2\right) + E_{hj}^2 E_{gj}^2. \qquad (25)$$

Then the complete complex dielectric function of the material of the carbon-nitride thin films is given as follows [17]:

$$\hat{\varepsilon}(E) = 1 + \sum_{j=1}^{N} \hat{\varepsilon}_{j\to j^*}(E), \qquad (26)$$

where

$$\hat{\varepsilon}(E) = \varepsilon_r(E) + \mathrm{i}\varepsilon_i(E) \qquad (27)$$

and

$$\hat{\varepsilon}_{j\to j^*}(E) = \varepsilon_{r,j\to j^*}(E) + \mathrm{i}\varepsilon_{i,j\to j^*}(E). \qquad (28)$$

The refractive index $n_1(E)$ and extinction coefficient $k_1(E)$ are connected with the real part $\varepsilon_r(E)$ and imaginary part $\varepsilon_i(E)$ of the dielectric function by means of the following equations:

$$\varepsilon_r(E) = n_1^2(E) - k_1^2(E) \qquad (29)$$

and

$$\varepsilon_i(E) = 2n_1(E)k_1(E). \qquad (30)$$

By using (29) and (30), it is possible to calculate the spectral dependences of the refractive index $n_1(\lambda)$ and the extinction coefficient $k_1(\lambda)$ of the thin films under study because $\lambda = hc/E$, where $c$ is the velocity of light in vacuum.

From the foregoing, it is obvious that using the LSM, the values of the local thickness $d^{k,u}$ and material parameters, i.e. the parameters $E_{gj}$, $E_{hj}$ and $Q_j$ occurring in the dispersion model used, are determined for each local area. Using these material parameters, one can calculate the true spectral dependences of the refractive index and the extinction coefficient of the carbon-nitride films within the local areas corresponding to the pixels of the CCD camera. This means that the distributions (maps) of the thickness and optical constants are determined in this way. The spectral dependences of the optical constants of the silicon single

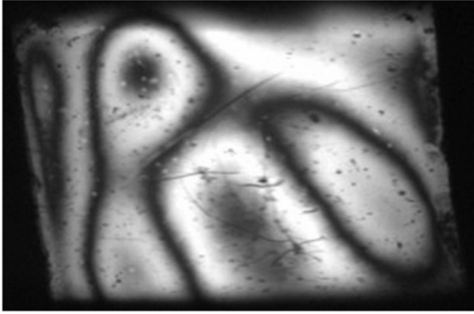

**Figure 2.** Image of the film investigated for the wavelength of 440 nm.

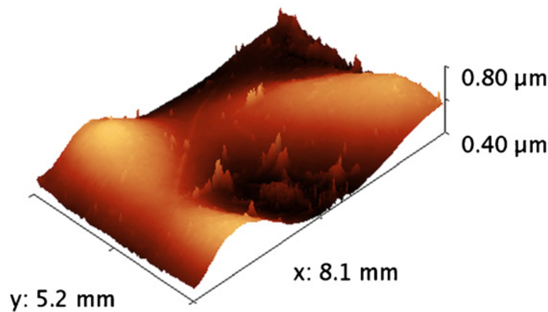


**Figure 3.** The 3D distribution of the local thickness of the carbon-nitride film selected determined using the ISR method.

crystal substrates were taken from the literature [18] and fixed within the LSM employed.

## 4. Results and discussion

It was found that the best fit of the experimental data belonging to individual pixels was achieved for the dispersion model corresponding to two transitions of electrons, i.e. for $N = 2$ (see equations (14) and (26)). The results presented in this paper represent typical results of the optical characterization of non-uniform carbon-nitride films studied using ISR. These results were achieved for the film prepared using the ratio $CH_4$:$N_2$ = 1:10. In figure 2, the image of this carbon-nitride film obtained by the CCD camera is presented for the wavelength of 440 nm.

In figure 3, the local thickness distribution of the carbon-nitride film selected is presented.

This distribution corresponds to the CCD camera image presented in figure 2. It was determined using the procedure of ISR presented above. Of course, the same local thickness distribution corresponded to images belonging to other wavelengths exhibiting different area distributions of the local reflectance values from that shown in figure 2. From figure 3, it is seen that the film exhibited relatively strong thickness non-uniformity. For the film selected, it was found that the values of the material parameters of the dispersion model were practically identical for all the local areas belonging to individual pixels. Thus, the non-uniform

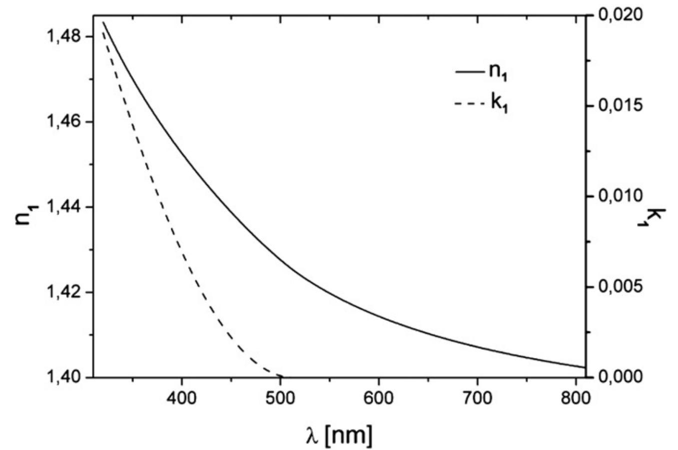


**Figure 4.** Spectral dependences of the refractive index $n_1$ and extinction coefficient $k_1$ of the non-uniform carbon-nitride film selected.

carbon-nitride film selected exhibited area uniformity in the material parameters. The values of these material parameters were found to be as follows:

$$E_{g1} = (2.42 \pm 0.03)\ \text{eV}, \quad E_{g2} = (11.34 \pm 0.08)\ \text{eV},$$
$$E_{h1} = (44.81 \pm 0.06)\ \text{eV}, \quad E_{h2} = (12.1 \pm 0.6)\ \text{eV},$$
$$Q_1 = (32.9 \pm 0.7)\ \text{eV}^{3/2}, \quad Q_2 = (66.6 \pm 0.9)\ \text{eV}^{3/2}.$$

This means that this film was also uniform in the optical constants along the area of the film. The spectral dependences of the refractive index $n_1(\lambda)$ and extinction coefficient $k_1(\lambda)$ of the film calculated using the values of the material (dispersion) parameters introduced above are plotted in figure 4. From this figure it is clear that the carbon-nitride film is an absorbing film for a shorter wavelength of 500 nm. For longer wavelengths this film is non-absorbing. Note that the remaining carbon-nitride films studied exhibited evident thickness non-uniformity.

The correctness of the results obtained within the optical characterization performed for the sample of the selected carbon-nitride film is supported by the good agreement between the experimental and theoretical data. This fact is illustrated for the pixel selected in figure 5. Note that the theoretical data were calculated using equation (8) on the basis of the values of the parameters found using the LSM. The good agreement between both the theoretical and experimental data also indicates that the film under study was uniform in optical parameters within the area imaged by our spectrophotometer onto one pixel of the CCD camera, i.e. within the area of $37 \times 37\ \mu\text{m}^2$. In the opposite case, this good agreement could not be achieved. In particular, the differences between the experimental and theoretical values of the extremes in the spectral dependences of the local reflectance should be observed then. The foregoing statements concerning the local uniformity of the film characterized are evident if one realizes that the theoretical values of local reflectance were calculated using the formula valid for the uniform slightly absorbing thin film. Note that the same good agreement between both the experimental and theoretical data of the sample characterized was also achieved for the remaining pixels of the CCD camera.

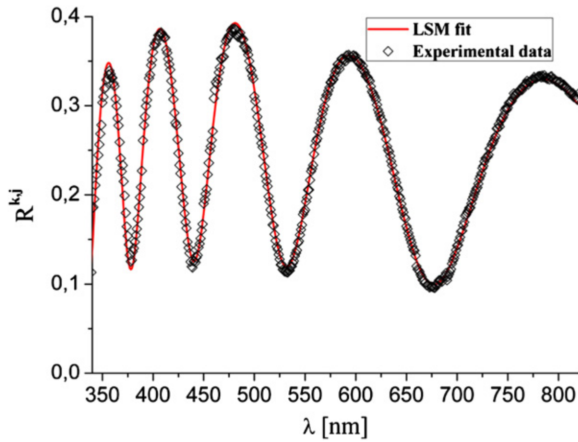


**Figure 5.** Spectral local reflectance of the carbon-nitride film under study corresponding to the selected pixel: the points denote the experimental values and the curve represents the theoretical data.

The local reflectance values $R^{k,u}$ were measured with the relative accuracy of about 1%. Using a standard error analysis, we found that the values of the local thicknesses in the area distributions were determined with a relative accuracy of 1–2%. The same conclusion concerning the accuracy was established for the optical constants. Note that the precision presented above corresponds to the statistical precision.

In conclusion, it should be pointed out that the transition characterized by the material parameters $E_{g2} = 11.34$ eV, $E_{h2} = 12.1$ eV and $Q_2 = 66.6$ eV$^{3/2}$ probably does not represent a real transition. This statement is mainly supported by the high value of $E_{g2}$. We therefore believe that the second transition ($j = 2$) probably compensates some systematic error occurring in the experimental data. We believe that the influence of a certain nonlinearity of the CCD camera or the influence of a light intensity background can cause this systematic error in the experimental data. An analysis of the systematic errors concerning the experimental data obtained for the individual pixels of the CCD camera will be presented elsewhere. However, the values of the material parameters of the second transition indicate that the systematic error considered cannot be important, which is implied by the fact that the contribution of $\hat{\varepsilon}_{2\rightarrow 2^*}(E)$ to $\hat{\varepsilon}(E)$ calculated using these values of the material parameters is relatively small. Of course, the first transition ($j = 1$) represents the real transition.

It should be noted that by means of ISR, similar results for the optical characterization of the other carbon-nitride films prepared by the same technological procedure as that for the film studied here were obtained.

In conclusion, the following advantages and limitations of the presented ISR method are summarized.

(1) In principle, the method can be applied to the complete optical characterization of thin films exhibiting area non-uniformity in thickness and optical constants simultaneously.
(2) Relatively large areas of the non-uniform thin films can be characterized as the consequence of imaging this relatively large film area onto the CCD chip (in our ISP, it is possible to imagine thin film areas up to 1 cm$^2$).
(3) No limiting assumptions must be put on thin film area non-uniformity if it is fulfilled that the local reflectance of the film areas imagined onto individual pixels corresponds to the reflectance of uniform thin films with a sufficient accuracy. This means that general area non-uniformity in the optical parameters of the thin films can be studied under fulfilling this condition. For example, no form of thickness non-uniformity must be assumed *a priori*. If the local reflectance values cannot be approximated by the reflectance of the uniform thin films, the procedure of ISR presented here has to be modified (this modification will be presented elsewhere too).
(4) Films exhibiting a relatively strong non-uniformity in thickness and optical constants can be characterized using this method (see figure 3).
(5) Within this ISR method, the dispersion models of the optical constants of the non-uniform thin films characterized can be used so that the values of materials parameters of these films such as band gap can be determined too. These dispersion models need not be known *a priori* because they can be modeled and specified by fitting the local reflectance data in the same way as is performed by fitting the experimental data obtained by the standard optical methods such as spectroscopic ellipsometry (see e.g. [7, 8, 17]).
(6) In principle, the application of the method does not depend on the structural properties of the analyzed non-uniform thin films. Thus, the method can be applied to characterizing amorphous, polycrystalline, single crystalline and nano-structured non-uniform thin films. Of course, suitable dispersion models must be used to perform a successful and reliable characterization of the individual films mentioned above.

The main limitations of the described ISR method are as follows.

(1) The method is suitable for characterizing thin films having a sufficiently low absorption within the spectral region employed in the ISP. In other words, using the method presented here, non-uniform thin films, both the boundaries of which influence the measured local reflectance, can be characterized using this method. If absorption of the non-uniform film is too strong within the spectral region considered and the lower boundary has no influence on the local reflectance, then the method is not usable for characterizing such films since it is impossible to determine the values of the local thickness. Thus, the method of ISR presented here is efficient for dielectric and semiconductor thin films. For strongly absorbing thin films such as metal films, this method is not usable practically.
(2) If the dispersion model of the non-uniform thin film characterized is complicated and contains a large number of parameters, it is often impossible to determine the values of all these parameters together with the local thickness value by means of ISR in the consequence of their mutual correlation within the LSM. In this case, it is necessary to combine this method together with auxiliary optical methods, for example, with standard spectroscopic ellipsometry or standard spectroscopic photometry.

## 5. Conclusion

In this paper, a new original method for the optical characterization of non-uniform slightly absorbing thin films based on imaging spectroscopic reflectometry (ISR) was presented. An original imaging spectroscopic photometer (ISP) operating in reflection mode was employed for obtaining the experimental data. The spectral dependences of the normal local reflectance corresponding to the individual pixels of the CCD camera serving as the detector of the ISP were treated using the LSM. Within the LSM, the formula for the normal local reflectance of the uniform absorbing thin film placed on an absorbing substrate was used. When treating the experimental data, the dispersion model based on the parameterization of the joint density of electronic states corresponding to amorphous materials was used. It was shown that in principle it is possible to determine both the thickness and optical constant distributions simultaneously in an independent way. This fact represents an important advantage of this method. Moreover, it was shown that using this method it is possible to determine the values of the dispersion (material) parameters of the films characterized in principle. The method was applied to the optical characterization of the non-uniform carbon-nitride films deposited by the dielectric barrier discharge method onto the silicon single crystal substrates. Using this method, the local thickness distributions were determined for these films. Furthermore, it was shown that the carbon-nitride films were uniform in optical constants. The spectral dependences of the optical constants and area distributions of the local thickness for the carbon-nitride film selected were presented. It was also presented that the local thickness values and spectral dependences of the optical constants of the carbon-nitride films were determined with relatively high accuracy. From this paper it is clear that the method of the ISR described here is also usable for the optical characterization of other non-uniform absorbing thin films described with different dispersion models (e.g. for the dispersion model presented in [19]). Of course, the method can be successfully utilized for the complete optical characterization of non-uniform non-absorbing thin films. In the paper, the practical advantages and limitations of the ISR method presented are also summarized. It should be noted that non-uniform thin films often exhibit miscellaneous defects such as boundary roughness (see e.g. [20]), optical inhomogeneity represented by a refractive index profile across the film (see e.g. [20, 21]), volume inhomogeneity corresponding to columnar structure (see e.g. [22]), etc. These defects can be included in the formulae for the local reflectance of non-uniform thin films in a relatively easy way. It will be performed in our forthcoming papers. However, on the basis of these formulae the optical characterization of non-uniform thin films containing other defects using ISR can often be very complicated or ambiguous (this statement is especially true if the defects are combined). In this case it is necessary to use some auxiliary methods. For example, within the optical characterization of the non-uniform thin films exhibiting columnar structure, it will be reasonable to combine ISR with atomic force microscopy because this technique enables us to analyze thin film columnar structure quantitatively (see [23]). Examples of the optical characterization of non-uniform thin films exhibiting further defects will also be presented in our forthcoming papers.

## Acknowledgments

This work was supported by the Ministry of Education, Youth and Sports of the Czech Republic under contracts MSM 0021630518 and MSM 0021622411 and the Ministry of Industry and Trade of the Czech Republic under contracts FR-TI1/168 and FT-TA5/114.

## References

[1] Pisarkiewicz T, Stapinski T, Czternasek H and Rava P 1991 Inhomogeneity of amorphous-silicon thin-films from optical-transmission and reflection measurements *J. Non-Cryst. Solids* **137/138** 619–22

[2] Pisarkiewicz T 1994 Reflection spectrum for a thin-film with nonuniform thickness *J. Phys. D: Appl. Phys.* **27** 160–4

[3] Majumdar A, Schäfer J, Mishra P, Ghose D, Meichsner J and Hippler R 2007 Chemical composition and bond structure of carbon-nitride films deposited by $CH_4/N_2$ dielectric barrier discharge *Surf. Coat. Technol.* **201** 6437–44

[4] Török M I 1985 Determination of optical-constants of thin-films with non-uniform thickness from the fringe pattern of the transmittance spectra *Opt. Acta* **32** 479–83

[5] Gonzalez-Leal J M, Prieto-Alcon R, Vlcek M and Marquez E 2004 Structural and optical characterization of amorphous $As_{40}S_{60}$ and $As_{40}Se_{60}$ films prepared by plasma-enhanced chemical vapor deposition *J. Non-Cryst. Solids* **345** 88–92

[6] Howling A A, Sansonnens L, Ballutaud J, Hollenstein C and Schmitt J P M 2004 Nonuniform radio-frequency plasma potential due to edge asymmetry in large-area radio-frequency reactors *J. Appl. Phys.* **96** 5429–40

[7] Necas D, Ohlidal I and Franta D 2009 The reflectance of non-uniform thin films *J. Opt. A: Pure Appl. Opt.* **11** 045202

[8] Ohlidal I, Necas D, Franta D and Bursikova V 2009 Characterization of non-uniform diamond-like carbon films by spectroscopic ellipsometry *Diam. Relat. Mater.* **18** 364–7

[9] Ohlidal M, Ohlidal I, Klapetek P, Necas D and Bursikova V 2009 Application of spectroscopic imaging reflectometry to analysis of area non-uniformity in diamond-like carbon films *Diam. Relat. Mater.* **18** 384–7

[10] Ohlidal M, Cudek V, Ohlidal I and Klapetek P 2005 Optical characterization of non-uniform thin films using imaging spectrophotometry *Proc. SPIE* **5963** 596329

[11] Urbanek M, Spousta J, Behounek T and Sikola T 2007 Imaging reflectometry *in situ Appl. Opt.* **46** 6309–13

[12] Vašíček A 1960 *Optics of Thin Films* (Amsterdam: North-Holland)

[13] Knittl Z 1976 *Optics of Thin Films* (London: Wiley)

[14] Mott N F and Davis E A 1971 *Electronic Processes in Non-Crystalline Materials* (Oxford: Clarendon)

[15] Tauc J 1972 Optical properties of non-crystalline solids *Optical Properties of Solids* ed F Abelès (Amsterdam: North-Holland) pp 277–313

[16] Adachi S 1999 *Optical Properties of Crystalline and Amorphous Semiconductors: Materials and Fundamental Principles* (Boston, MA: Kluwer)

[17] Franta D, Necas D and Zajickova L 2007 Models of dielectric response in disordered solids *Opt. Express* **15** 16230–44

[18] Herzinger C M, Johs B, McGahan W A, Woollam J A and Paulson W 1998 Ellipsometric determination of optical constants for silicon and thermally grown silicon dioxide via multi-sample, multi-wavelength, multi-angle investigation *J. Appl. Phys.* **83** 3323–26

[19] Franta D, Bursikova V, Ohlidal I, St'ahel P, Ohlidal M and Necas D 2007 Correlation of thermal stability of the mechanical and optical properties of diamond-like carbon films *Diam. Relat. Mater.* **16** 1331–5

[20] Ohlidal I, Navratil K and Ohlidal M 1995 Scattering of light from multilayer systems with rough boundaries *Progress in Optics* vol 34 ed E Wolf (Amsterdam: Elsevier) pp 249–331

[21] Franta D and Ohlidal I 2000 Optical characterization of inhomogeneous thin films of $ZrO_2$ by spectroscopic ellipsometry and spectroscopic reflectometry *Surf. Interface Anal.* **30** 574–9

[22] Ohlidal I and Navratil K 1980 Determination of the optical-parameters and packing density of non-absorbing columnar thin-films by means of immersion reflectometry—application to LiF thin-films *Thin Solid Films* **74** 51–8

[23] Klapetek P, Ohlidal I and Bursik J 2007 Atomic force microscopy studies of cross-sections of columnar thin films *Meas. Sci. Technol.* **18** 528–31